forests

MDPI

Article

Enhancement of Dimensional Stability, Hydrophobicity, and Mechanical Strength of North American Red Alder Wood Through Silane Impregnation Combined with DES Pretreatment

Yang Zheng [1,2], Ting Zhou [2], Chenyang Cai [1,2] and Honghai Liu [1,2,*]

[1] Jiangsu Co-Innovation Center of Efficient Processing and Utilization of Forest Resources, Nanjing Forestry University, Nanjing 210037, China; chenyangc@hotmail.com (C.C.)
[2] College of Furnishings and Industrial Design, Nanjing Forestry University, Nanjing 210037, China
* Correspondence: liuhonghai2020@njfu.edu.cn

Abstract

Wood is a green and renewable bio-based building material, but its hygroscopicity affects its dimensional stability, limiting its use in construction. Chemical modification can improve its properties, yet its effectiveness depends on wood permeability and traditional modifiers. This study first used a deep eutectic solvent (DES) to boost the permeability of North American alder wood. Then, methyl trimethoxysilane was impregnated under supercritical carbon dioxide (SCI), pressure (PI), vacuum (VI), and atmospheric pressure (AI) conditions. DES treatment damaged the cell structure, increasing wood permeability. Silane was deposited and polymerized in the cell lumen, chemically bonding with cell-wall components, filling walls and pits, and thickening walls. The VI group had the highest absolute density (0.59 g/cm^3, +36.6%) and the lowest moisture absorption (4.4%, −33.3%). The AI group had the highest ASE (25%). The PI group showed the highest surface hardness (RL, 2592 N) and a water contact angle of 131.9°, much higher than natural wood. Overall, the VI group had the best performance. Silane reacts with cellulose, hemicellulose, and lignin in wood via hydrolysis and hydroxyl bonding, forming stable bonds that enhance the treated wood's hydrophobicity, dimensional stability, and surface hardness.

Keywords: deep eutectic solvent (DES); silane impregnation; wood modification; dimensional stability; hydrophobicity

check for updates

Academic Editor: Tripti Singh

Received: 8 June 2025
Revised: 6 July 2025
Accepted: 11 July 2025
Published: 12 July 2025

Citation: Zheng, Y.; Zhou, T.; Cai, C.; Liu, H. Enhancement of Dimensional Stability, Hydrophobicity, and Mechanical Strength of North American Red Alder Wood Through Silane Impregnation Combined with DES Pretreatment. *Forests* **2025**, *16*, 1152. https://doi.org/10.3390/f16071152

Copyright: © 2025 by the authors. Licensee MDPI, Basel, Switzerland. This article is an open access article distributed under the terms and conditions of the Creative Commons Attribution (CC BY) license (https://creativecommons.org/licenses/by/4.0/).

1. Introduction

Since ancient times, people have favored wood as a building material due to its natural advantages, such as its exceptional strength-to-weight ratio, heat insulation, ease of processing, and superior seismic performance [1]. Nowadays, with increasing emphasis on environmentally friendly and sustainable development practices, wood remains widely used in modern construction engineering as a green and renewable material. However, wood's physical and chemical properties, including its susceptibility to moisture, which can lead to swelling, deformation, and degradation, limit its use in wooden buildings [2,3]. Therefore, enhancing wood's performance and extending its service life through functionalization has become a significant area of research. However, most wood has low permeability, preventing the migration of modifying agents into the wood, which lowers the efficiency of the modification process.

Pretreatment methods can enhance wood permeability, establishing effective channels for modifier migration [4]. This step is pivotal in preparing wood for subsequent modifica-

tions. Traditional methods encompass physical, chemical, and biological approaches such as steam explosion, acid–base treatment, and microbial decomposition [5–9]. These techniques eliminate non-cellulosic components, increase porosity and surface roughness, and enhance the penetration and effectiveness of modifiers; however, they may have limited effectiveness in improving permeability or could have negative environmental impacts. Deep eutectic solvents (DESs), a novel class of eco-friendly solvents, have garnered attention for their low volatility, customizable properties, straightforward preparation, cost-effectiveness, and biodegradability [10]. DESs effectively disaggregate and transform biomass components, particularly lignin and hemicellulose, demonstrating considerable potential in wood pretreatment. Presently, DESs find application in wood modification, delignification, pretreatment, and wood fiber modification [8,9,11–14]. By dissolving lignin and altering wood pore structure, DESs can modify wood properties and enhance permeability. Adjusting DES treatment conditions enables precise control over wood treatment [4,15], facilitating customized modifications. Compared with conventional chemicals, DESs offer advantages of affordability, non-toxicity, and recyclability [16].

Wood chemical modification effectively alters its composition and properties but can be complex and may result in by-product pollution. Many chemical modifiers exhibit poor compatibility with wood cell walls, limited swelling ability, and difficulty penetrating wood cell walls, thereby contributing minimally to dimensional stability. In contrast, silane modification stands out because it enhances wood's hydrophobicity, antibacterial properties, and weather resistance through the formation of stable chemical bonds with hydroxyl groups on wood fibers [17]. Silane modification is environmentally friendly and enhances both the physical and chemical stability of wood, improving corrosion resistance, oxidation resistance, and antibacterial resistance, offering precise control over its properties [18–21].

DES pretreatment can create new liquid transfer channels in the multi-level pores of the wood cell walls, significantly improving the liquid permeability of wood. As a result, it effectively enhances the rate and efficiency of the impregnation of silane modifiers. This approach combines the advantages of DES pretreatment and silane modification, enhances its potential for broader applications, and compensates for the deficiencies of single-modification methods. This study examines how the integration of DES pretreatment and silane modification affects various properties of North American alder wood, including water absorption, moisture absorption, dimensional stability, hardness, hydrophobicity, microstructure, and chemical structure. The goal is to provide new insights into the effective functional modification of wood, thereby broadening its application scope in the wood industry.

2. Materials and Methods

2.1. Materials and Chemicals

The kiln-dried North American alder (*Alnus rubra* f. *pinnatisecta*) boards measuring 20 mm × 20 mm × 1000 mm (R × T × L) were supplied by Chongqing Mage Company (Chongqing, China). They were delivered to Nanjing Forestry University. Then, two boards were selected for cutting specimens with dimensions of 20 mm × 20 mm × 20 mm (R × T × L). In this experiment, there were 5 groups of test specimens (Table 1), with 10 specimens in each group, resulting in a total of 50 specimens. Choline chloride powder (AR, 98%), lactic acid (AR, 90%), methyltrimethoxysilane (AR, 99%), acetic acid (AR, 99%), and ethanol (AR, 95%) were procured from China National Pharmaceutical Group Chemical Reagent Co., Ltd. (Shanghai, China) Pure water was prepared in-house at the laboratory.

Table 1. Experimental groups and impregnation conditions.

Groups	Code	DES Pretreatment	Silane Impregnation	Impregnation Conditions
0	NW	No	No	No
1	SCI	Yes	Supercritical CO_2	10 MPa/25 °C/4 h
2	PI	Yes	Pressure	2.5 MPa/25 °C/4 h
3	VI	Yes	Vacuum	−0.1 MPa/25 °C/4 h
4	AI	Yes	Atmospheric	0.1 MPa/25 °C/4 h

2.2. Wood DES Pretreatment

The wood pretreatment method involves treating with a low-melting solvent composed of choline chloride and lactic acid. The treatment process is conducted at 80 °C, with a DES volume fraction of 50%, using a ratio of N (ChCl) to n (LA) of 1:6. The optimal treatment time is 6 h determined by pre-tests.

2.3. Preparation of the Silane Hydrolysis Solution

To enhance the reaction performance of silane modifiers, it is essential that the silane solution is hydrolyzed. The procedure is as follows: For each modified solution, 80 g of methyltrimethoxysilane is added to 200 mL of an 80% ethanol aqueous solution (160 mL ethanol and 40 mL pure water). The pH is adjusted to 4.0–4.5 using acetic acid. The solution is magnetically stirred at 1200 rpm at room temperature for 3 h to obtain the hydrolyzed silane solution.

2.4. Preparation of Modified Specimens

To investigate the impact of various treatment methods on the efficacy of silane impregnation, four impregnation approaches were applied to pretreated specimens: supercritical carbon dioxide-assisted impregnation (SCI), pressure impregnation (PI), vacuum impregnation (VI), and atmospheric pressure impregnation (AI). The control group was the natural wood (NW) without any treatment, (Table 1). Each group consisted of 10 samples.

2.5. Weight Percentage Gain

Weight percentage gain (WPG) following silane impregnation was calculated based on the mass changes using small samples measuring 20 mm × 20 mm × 20 mm (R × T × L), as in Equation (1).

$$WPG = (M_i - M_0)/M_0 \times 100 \quad (1)$$

where M_0 (g) and M_i (g) represent the oven-dried mass of specimens before and after silane impregnation, respectively.

2.6. Density

Wood density was determined using the Method for Determining Wood Density (GB/T1933-2009) [22]. Since wood density varies with the moisture content of specimens, the oven-dry density (ρ_0) was calculated using Equation (2) to assess the impact of the modification.

$$\rho_0 = M_0/V_0 \quad (2)$$

where M_0 is the absolute dry mass (g) and V_0 is the absolute dry volume (cm^3).

2.7. Moisture Absorption and Water Uptake

Moisture absorption and water uptake were determined following the guidelines of GB/T-1931-2009 [23], using absolute dried specimens measuring 20 mm × 20 mm × 20 mm (R × T × L). For water adsorption, initial measurements of mass and dimensions were

taken in the tangential, radial, and longitudinal directions. Subsequently, the samples were conditioned in a chamber at 20 ± 2 °C with 60 ± 5% relative humidity (RH) until reaching constant weight. Throughout the conditioning, measurements of mass and dimensions were taken using an electronic balance and digital caliper. For the water uptake test, an additional 6 groups of specimens (10 replicates) were submerged in distilled water within a plastic box. Similar to the water adsorption test, measurements of mass and dimensions were taken during the water uptake process. Upon reaching constant weight, all specimens were re-measured for mass and dimensions after cleaning the water from their surfaces. The moisture content of specimens during these processes was calculated using Equation (3).

$$\text{Moisture content (MC)} = (M_f - M_0)/M_0 \times 100 \quad (3)$$

where M_f is the mass after adsorption or water uptake (g) and M_0 is the absolute dry mass (g).

2.8. Anti-Swelling Efficiency (ASE)

ASE is an important indicator for measuring the improvement of the dimensional stability of wood after treatment. ASE was calculated using Equations (4) and (5).

$$S = (V_f - V_0)/V_0 \times 100 \quad (4)$$

where S is the volumetric swelling ratio of wood after treatment, V_f is the volume after adsorption or water uptake (cm^3), and V_0 is volume at the absolute dry state (cm^3).

$$\text{ASE} = (S_0 - S_t)/S_0 \times 100 \quad (5)$$

where S_t is the volume swelling coefficient of the treated wood and S_0 is the volume swelling coefficient of the control group.

2.9. Hardness of Specimens

The determination of specimen hardness follows the Test Method for Wood Hardness (GB/T 1927.19-2021) [24]. Select small specimens ((20 mm × 20 mm × 20 mm (R × T × L)) without defects such as cracks and knots. Fix the specimen perpendicular to the grain (RL) on the support of the testing machine. Use a hemispherical steel indenter (with a radius of 5.64 ± 0.01 mm) to aim at the center of the specimen, and press it into the surface at a uniform speed of 3–6 mm/min to a depth of 5.64 mm (for specimens prone to cracking, the depth can be reduced to 2.82 mm).

2.10. Water Contact Angle

A droplet shape analyzer (DSA100S, KRUSS Industry Co., Ltd., Hamburg, Germany) was employed to measure time-dependent contact angles using the sessile drop method. All specimens were conditioned at 20 ± 2 °C with 60 ± 5% RH until reaching constant weight. Subsequently, 5 μL of distilled water was dropped onto the transverse section of the specimens, and contact angle data were recorded. The average contact angle was measured by testing three different positions on the surface of the same sample.

2.11. Fourier-Transform Infrared Spectrometer (FTIR)

The chemical structure changes of the specimens were assessed using Fourier-transform infrared spectroscopy (FTIR, VERTEX 80v, Bruker, Rheinstetten, Germany) at a spectral resolution of 4 cm^{-1} with 16 scans. Wood powder samples were analyzed via diffuse reflectance in the 4000–400 cm^{-1} region.

2.12. Scanning Electron Microscopy (SEM)

To observe the microstructure, specimens measuring 5 mm × 5 mm × 5 mm (R × T × L) were prepared and freeze-dried until reaching constant weight. Subsequently, they were affixed to conductive adhesives and coated with gold. The SEM analysis (FEI Quanta 200, Eindhoven, The Netherlands) allowed observation of both tangential and transverse sections of the specimens.

3. Results and Discussion

3.1. Weight Percentage Gain and Density

Figure 1A illustrates that specimens impregnated with silane using SCI had the lowest WPG at only 0.5%. In contrast, specimens impregnated with silane using PI and AI showed weight gain rates of 15.5% and 13.8%, respectively. VI impregnation resulted in a higher WPG of 28.1%. The notably low WPG of SCI specimens may be attributed to the escape of high-pressure carbon dioxide during the pressure relief stage, which could lead to the removal of both the silane already bonded to the wood and the extractives present in the wood. Additionally, structural alterations induced by DES pretreatment might have reduced the efficiency of the silane–wood binding, leading to further loss of silane during this stage [25,26].

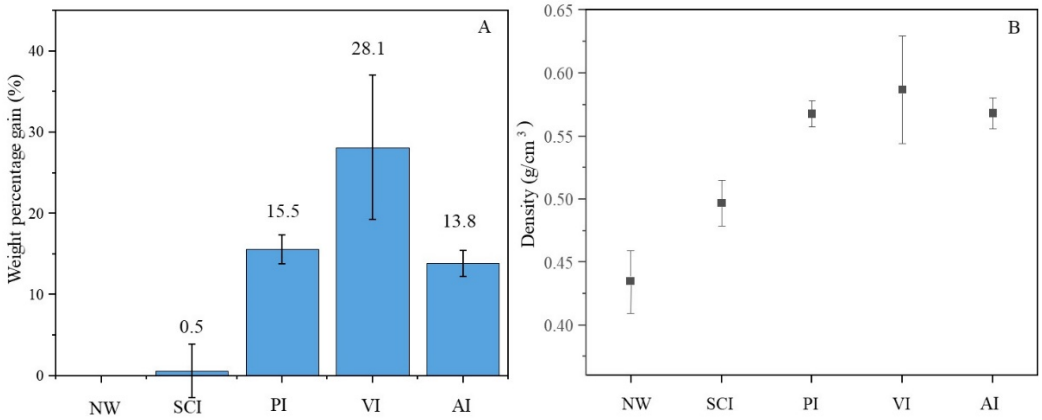


Figure 1. WPG (**A**) and oven-dry density (**B**) of untreated control wood and silane-impregnated specimens.

Figure 1B illustrates the variation in absolute dry density among the impregnated specimens and natural wood. The absolute dry density of these specimens is significantly higher than that of North American alder wood. The density growth rates for the SCI, PI, VI, and AI groups were relatively high, at 15.6%, 32.3%, 36.6%, and 32.3%, respectively, which aligns with the density trends observed in Figure 1A. The density of all other groups increased following silane impregnation, indicating successful impregnation and contributing to the overall density increase [27].

3.2. Moisture Absorption and Dimensional Stability

Figure 2A,B show the MC and volume change curves for natural wood and impregnated specimens during the absorption process, while Figure 2C,D illustrate their MC and ASE after 40 h of absorption. The NW group exhibited the lowest MC and volume at the early stages of absorption, but both parameters increased from 18 h onward, reaching their highest levels after 40 h (MC = 6.6%, volume change = 2.0%). This is because the wettability of wood is time-dependent. In the initial stage, water is only adsorbed on the surface or the shallow cell walls. Sufficient energy (such as breaking hydrogen bonds) needs to be accumulated for water to penetrate into the deep-seated structure. The MC of the SCI, PI, VI, and AI groups decreased by 17.7%, 22.7%, 33.3%, and 28.8%, respectively, with the VI

group showing the lowest MC of 4.4%. Meanwhile, the ASEs for the SCI, PI, VI, and AI groups are 5%, 10%, 15%, and 25%, respectively, with the AI group having the highest ASE of 25%. These results indicate that silane impregnation significantly reduces moisture absorption capacity and enhances the dimensional stability of the wood [28].

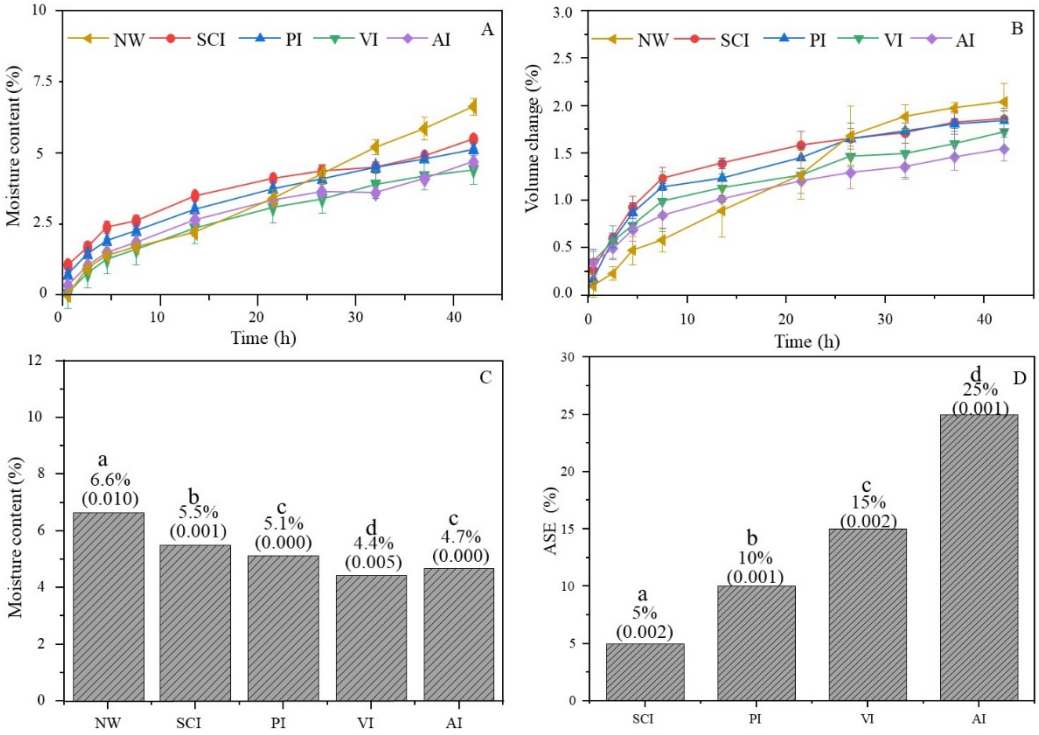


Figure 2. Changes curves of MC (**A**) and volume (**B**) of natural wood and silane-impregnated specimens during water absorption and comparisons of MC (**C**) and ASE (**D**) after 40 h water absorption. According to Duncan's multiple comparison test, the error bars with different letters indicate significant differences ($p < 0.05$).

3.3. Water Uptake and Dimensional Stability

Figure 3A,B display the MC and volume change curves for natural wood and impregnated specimens during the water uptake process, while Figure 3C,D illustrate their MC and ASE after 10 h of water uptake. The water uptake rate was rapid across all specimens during the first 10 min, with the SCI group reaching approximately 30% MC, followed by the NW group at around 20% MC, while the MC for the other groups was about 10%. Despite the high water uptake in the early stages by the SCI and NW groups, their volume change was not the highest, particularly for the NW group, which had the lowest volume change. After 10 h of water uptake, the MC of the impregnated specimens increased significantly compared with the NW group, with the SCI group showing the highest MC of 83%. In addition, the volume of all impregnated specimens increased significantly. Among them, the volume of the specimens in the AI group increased the most (38%), while the increases in the SCI and VI groups (23%) were much smaller compared with that of the AI group. SCI and VI may reduce extractives and improve wood permeability [29], contributing to increased MC without significantly affecting dimensional changes. These results indicate that silane impregnation negatively impacts MC and dimensional changes during the wood water uptake process.

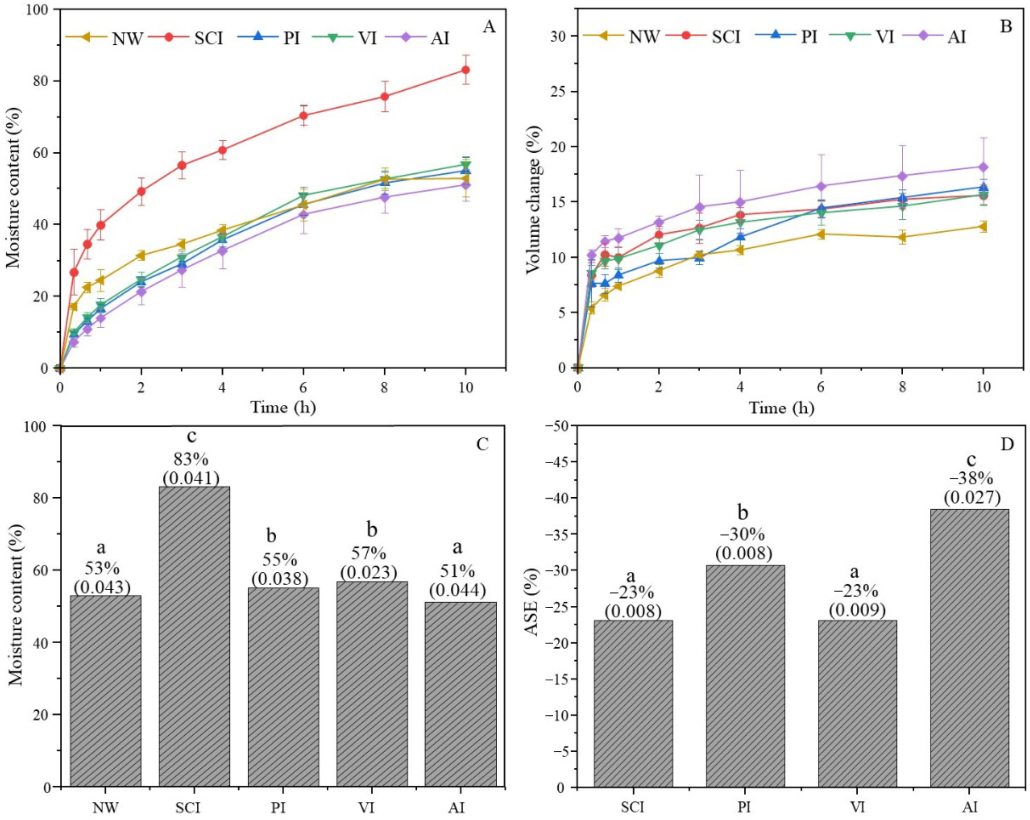


Figure 3. Changes curves of MC (**A**) and volume (**B**) of untreated control wood and silane-impregnated specimens during water uptake and comparisons of MC (**C**) and ASE (**D**) after 10 h of water uptake. According to Duncan's multiple comparison test, the error bars with different letters indicate significant differences ($p < 0.05$).

3.4. The Effect of Silane Impregnation on the Surface Hardness of Specimens

Figure 4 illustrates the changes in surface hardness of wood perpendicular to the grain (RL) and Duncan's multiple comparison ($p < 0.05$). Surface hardness is measured by the force required to produce the same deformation on the wood surface. After silane impregnation, the hardness of the specimens increased significantly, with an average rise of 28% compared with the NW group. The PI group exhibited the highest surface hardness, with a value of 2592 N. PI forces small silane molecules (such as isooctyltriethoxysilane) to overcome the capillary resistance of the wood cell lumen and penetrate into the deep cell walls and pit structures. In the alkaline environment of wood, silane hydrolyzes into silanol (Si-OH), which condenses with the hydroxyl groups (-OH) of cellulose/hemicellulose to form Si-O-C covalent bonds. The high-pressure environment accelerates this reaction, increases the cross-linking density, and significantly enhances the rigidity of the cell walls. These findings suggest that silane impregnation improves surface hardness, but the effectiveness of the method varies, resulting in different degrees of improvement in wood surface hardness [30].

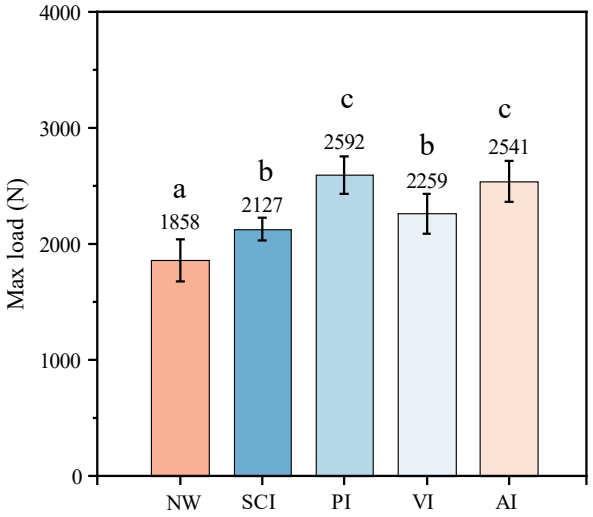


Figure 4. Surface hardness of untreated control wood and silane-impregnated specimens. According to Duncan's multiple comparison test, the error bars with different letters indicate significant differences ($p < 0.05$).

3.5. The Effect of Silane Impregnation on the Water Contact Angle of Specimens

Natural wood, with its high content of hydrophilic groups such as hydroxyl groups, typically exhibits strong hydrophilicity, with a contact angle normally smaller than 90° [31]. Following silane impregnation, all water contact angles were greater than 90° (Figure 5), indicating a significant enhancement in hydrophobicity. This is because the silane nanoparticles in the wood increase the surface roughness, which lowers the surface energy and makes it difficult for water droplets to spread out. Additionally, hydroxyl groups formed through chemical reactions bond with the existing hydroxyl groups in the wood, reducing their number and thus decreasing the wettability of the wood surface [32]. According to Figure 3A, during the water uptake process, the water absorption rates of PI and VI were lower than that of NW in the early stage, but higher than that of NW in the later stage. This may be due to the inadequate modification of silane, resulting in the incomplete filling of deep pores. The contact angle increases in the short term, but the water absorption rate rises after long-term immersion.

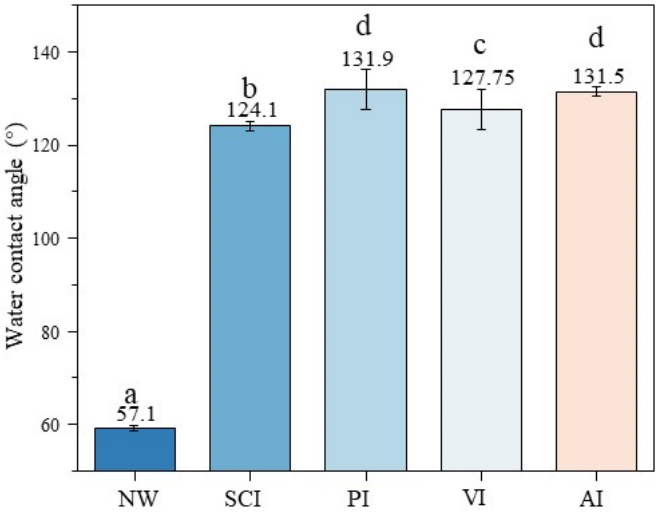


Figure 5. Water contact angle in cross section of untreated control and silane-impregnated wood. According to Duncan's multiple comparison test, the error bars with different letters indicate significant differences ($p < 0.05$).

3.6. The Effect of Silane Impregnation on the Chemical Composition of Specimens

Figure 6 displays the infrared spectrum of the specimen, revealing characteristic peaks of wood hydroxyl (-OH) groups between 3600 and 3100 cm^{-1}. The peak intensity indicates a reduction in hydroxyl groups after silane impregnation, suggesting the silane bonds with wood hydroxyl groups, thereby consuming some hydroxyl groups. This phenomenon contributes to enhancing the hydrophobicity of wood [33]. Near 2880 cm^{-1}, stretching vibrations of carbon–hydrogen bonds (C-H_2 and C-H_3) are observed in all samples. Additionally, silane impregnation introduces new methyl groups (-CH_3) alongside the inherent C-H bonds present in wood. At 1730 cm^{-1}, stretching vibrations of carboxylic acid groups (C=O) that have not undergone silanization can be observed. Between 1000 cm^{-1} and 1130 cm^{-1}, stretching vibrations of C-O bonds in wood lignin and asymmetric stretching vibrations of Si-O-Si and Si-O-C in siloxane were observed, indicating new chemical bonds introduced by silane impregnation. The tensile vibration and Si-C vibration in $SiCH_3$ near 578 cm^{-1} demonstrate the successful impregnation of methyltrimethoxysilane.

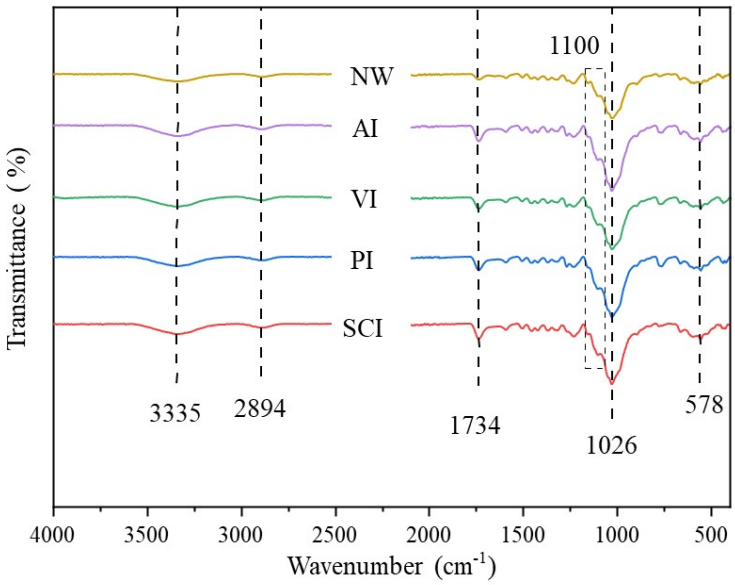


Figure 6. Infrared spectra of untreated control wood and silane-impregnated specimens.

3.7. The Effect of Silane Impregnation on the Microstructure of Specimens

Observation under a scanning electron microscope enables the exploration of the effects of DES pretreatment and silane impregnation on the microstructure of wood cell walls. As depicted in Figure 7A, the DES-pretreated sample shows clearly visible and open pit features. Conversely, in specimens after silane impregnation (Figure 7C), some pits appear blurred and blocked, indicating successful penetration and filling of micro-pores by silane, which may enhance the wood's hydrophobicity [34]. In Figure 7B, the cross section of the DES-pretreated specimens reveals that the cell wall becomes thinner with visible gaps, attributed to partial lignin removal from the wood by the DES. Following silane impregnation (Figure 7D), the wood cell wall thickens, and intercellular spaces and cell cavities experience compression and deformation to varying degrees. This occurs because silane reacts within the wood cell wall, binding to it and enabling in situ polymerization. DES pretreatment increases wood permeability, facilitating silane penetration into the wood interior and subsequent reactions [35].

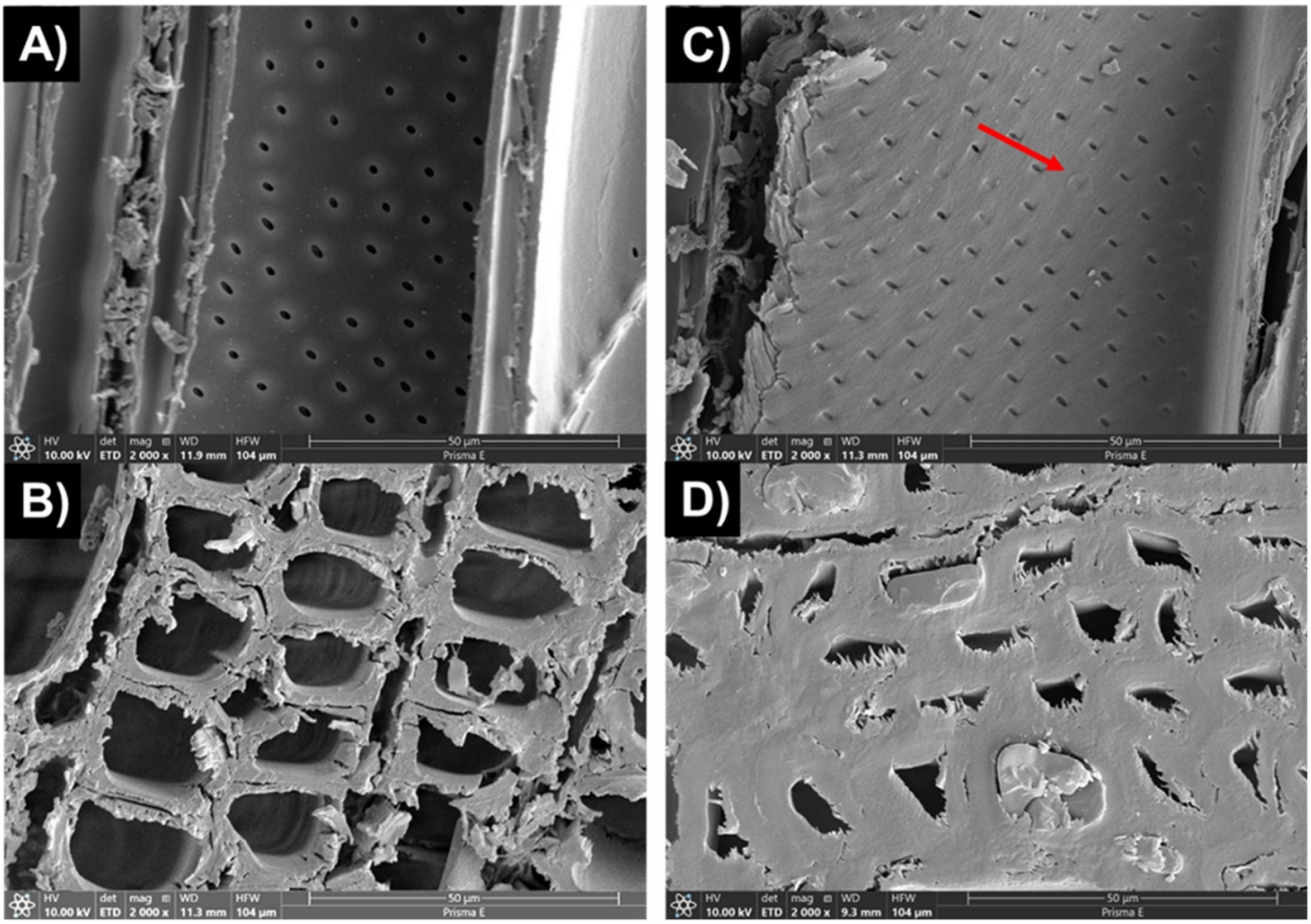


Figure 7. SEM images of DES-pretreated sample in tangential section (**A**) and transversal section (**B**); silane-impregnated specimens in tangential section (**C**) and transversal section (**D**).

3.8. The Mechanism of Silane Modification on Wood

Silanes and their derivatives can be applied in various environments, with temperature, pressure, and pH influencing their reactions to varying extents. In this experiment, the main reactions of silanes with wood involve two key aspects. The first aspect involves the hydrolysis of silane derivatives, where the resulting silanol forms more electrophilic and reactive hydrogen bonds. This stage can be managed by adjusting the solution composition, alcohols, water, and pH. The second aspect is the formation of hydrogen bonds between the hydrolyzed products and hydroxyl groups on the substrate, leading to the creation of covalent bonds during drying or curing, with water being released in the process (Figure 8) [36]. Currently, there is extensive research on the reaction mechanisms and expected effects between silane derivatives and other materials. Studies indicate that silanes primarily interact with the hydroxyl groups of cellulose in wood, forming chemical bonds through processes such as graft copolymerization. These interactions enhance hydrophobicity and improve the strength and other properties of wood. By designing effective chemical reactions involving silane derivatives, the performance of wood can be further enhanced [37–39].

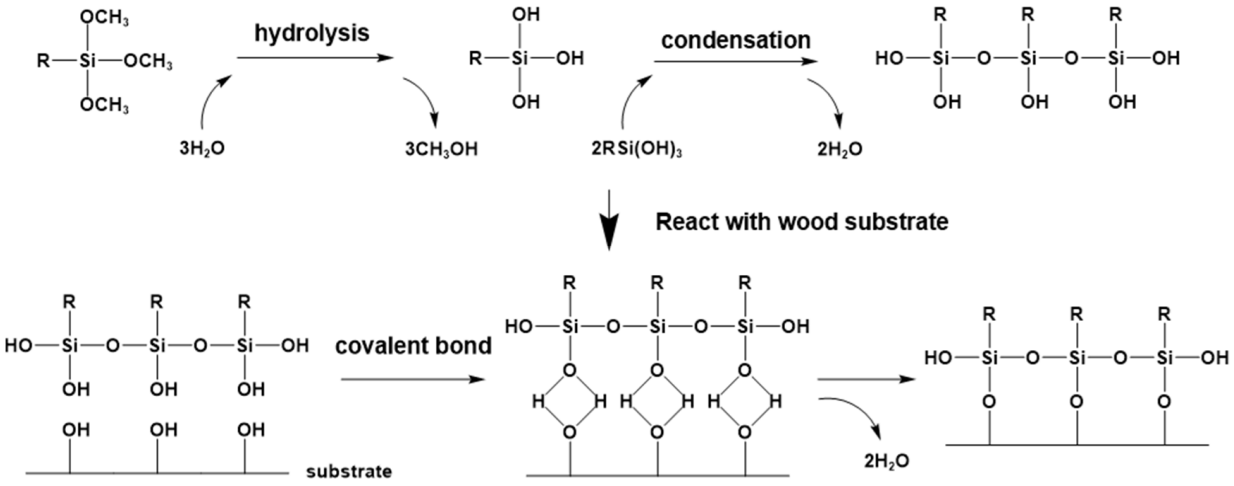


Figure 8. Schematic diagram of silane-modification mechanism.

4. Conclusions

This study successfully demonstrated the silane impregnation of wood pretreated with a deep eutectic solvent (DES), leading to significant improvements in hydrophobicity, dimensional stability, and surface hardness. The DES pretreatment effectively separated lignin from the wood, increasing its permeability and facilitating the silane impregnation. VI achieved the highest absolute density of 0.59 g/cm^3, an increase of 36.6%, and the lowest moisture absorption content of 4.4%, a decrease of 33.3%. AI resulted in the smallest absorption volume change of 1.5%, a decrease of 25.0%. However, silane impregnation did not reduce the moisture content and dimensional change upon water uptake. PI exhibited the highest surface hardness of 2592 N and a water contact angle of 131.9°, significantly higher than that of natural wood. Overall, wood treated with vacuum impregnation displayed the best properties. Silane was successfully deposited and polymerized in situ within the cell lumen, forming chemical bonds with the cell-wall components. This process filled the cell walls and pits, resulting in thickened cell walls. Additionally, the silane reacted with cellulose, hemicellulose, and lignin through hydrolysis and hydroxyl bonding, creating stable chemical bonds that significantly enhanced the wood's properties.

Author Contributions: Writing—original draft preparation, Y.Z. and T.Z.; writing—review and editing, C.C. and H.L.; All authors have read and agreed to the published version of the manuscript.

Funding: This work was supported by the National Natural Science Foundation of China Grant Nos. 32301521, 31870545, and 31570558.

Institutional Review Board Statement: Not applicable.

Informed Consent Statement: Not applicable.

Data Availability Statement: The original contributions presented in this study are included in the article. Further inquiries can be directed to the corresponding author.

Conflicts of Interest: The authors declare no conflicts of interest.

References

1. Yang, L.; Fan, H.; Zheng, J. Effect of Supercritical CO_2 Dehydration treatment on the *Juglans mandshurica*. *Wood Res.* **2025**, *70*, 212–223. [CrossRef]
2. Wang, X.; Yang, L. Effect of freezing and freezing-thawing pretreatment on wood properties and drying characteristics of *Eucalyptus urophylla* × *E.* grandis. *Wood Mater. Sci. Eng.* **2024**, 1–7. [CrossRef]
3. Yang, L.; Zhao, P.; Yin, Q. Study on The Hydrothermal Treatment of kiln-dried timber of Red Alder. *Wood Res.* **2025**, *70*, 224–236. [CrossRef]

4. Qi, Y.; Zhou, Z.; Xu, R.; Dong, Y.; Zhang, Z.; Liu, M. Effect of NaOH pretreatment on permeability and surface properties of three wood species. *ACS Omega* **2023**, *8*, 40362–40374. [CrossRef] [PubMed]
5. Xue, J.; Xu, W.; Zhou, J.; Mao, W.; Wu, S. Effects of high-temperature heat treatment modification by impregnation on physical and mechanical properties of poplar. *Materials* **2022**, *15*, 7334. [CrossRef]
6. Yang, L.; Li, S.; Han, Y. Effect of pre-freezing treatments on the drying behavior of *Eucalyptus platyphylla* FV Muell. *Drying Technology* **2025**, 1–10.
7. Wei, N.; Yang, C.; Su, Y.; Lai, C.; Yong, Q. Comparison of effects of carbocation scavengers assisted acid pretreatment on improving enzymatic digestibility of masson pine and poplar. *Ind. Crops Prod.* **2024**, *214*, 118603. [CrossRef]
8. Yang, Y.; Xu, W.; Liu, X.; Wang, X. Study on permeability of *Cunninghamia lanceolata* based on steam treatment and freeze treatment. *Wood Res.* **2021**, *66*, 721–731. [CrossRef]
9. Kwon, G.J.; Cho, S.W.; Bandi, R.; Yang, B.S.; Dadigala, R.; Han, S.Y.; Ma, S.Y.; Kim, J.K.; Kim, N.H.; Lee, S.H. Production of lignocellulose nanofibrils by conventional and microwave-assisted deep-eutectic-solvent pretreatments: Mechanical, antioxidant, and UV-blocking properties. *Cellulose* **2023**, *30*, 4277–4292. [CrossRef]
10. Troter, D.Z.; Todorović, Z.B.; Đokić-Stojanović, D.R.; Stamenković, O.S.; Veljković, V.B. Application of ionic liquids and deep eutectic solvents in biodiesel production: A review. *Renew. Sustain. Energy Rev.* **2016**, *61*, 473–500. [CrossRef]
11. Wu, Y.; Yang, L.; Zhou, J.; Yang, F.; Huang, Q.; Cai, Y. Softened wood treated by deep eutectic solvents. *ACS Omega* **2020**, *5*, 22163–22170. [CrossRef] [PubMed]
12. Ran, Y.; Lu, D.; Jiang, J.; Huang, Y.; Wang, W.; Cao, J. Deep eutectic solvents-assisted wood densification: A promising strategy for shape-fixation. *Chem. Eng. J.* **2023**, *471*, 144476. [CrossRef]
13. Malaeke, H.; Housaindokht, M.R.; Monhemi, H.; Izadyar, M. Deep eutectic solvent as an efficient molecular liquid for lignin solubilization and wood delignification. *J. Mol. Liq.* **2018**, *263*, 193–199. [CrossRef]
14. Fan, Z.; Sun, H.; Zhang, L.; Zhao, X.; Hu, Y. Lightweight, high-strength wood prepared by deep eutectic solvent treatment as a green structural material. *ACS Sustain. Chem. Eng.* **2022**, *10*, 9600–9611. [CrossRef]
15. Kroon, M.M.; Francisco Casal, M.M.; Bruinhorst, V.D.A.A. Pretreatment of Lignocellulosic Biomass and Recovery of Substituents Using Natural Deep Eutectic Solvents/Compound Mixtures with Low Transition Temperatures. Patent WO2013153203, 17 October 2013.
16. Xia, Q.; Chen, C.; Yao, Y.; Li, J.; He, S.; Zhou, Y.; Hu, L. A strong, biodegradable and recyclable lignocellulosic bioplastic. *Nat. Sustain.* **2021**, *4*, 627–635. [CrossRef]
17. Jamil, M.I.; Ali, A.; Haq, F.; Zhang, Q.; Zhan, X.; Chen, F. Icephobic strategies and materials with superwettability: Design principles and mechanism. *Langmuir* **2018**, *34*, 15425–15444. [CrossRef]
18. Ratajczak, I.; Woźniak, M.; Szentner, K.; Babicka, M.; Jenczyk, J.; Mazela, B. Aminosilane binding to wood substance through an alkyd resin. *J. Wood Chem. Technol.* **2020**, *40*, 73–79. [CrossRef]
19. Meints, T.; Hansmann, C.; Gindl-Altmutter, W. Suitability of different variants of polyethylene glycol impregnation for the dimensional stabilization of oak wood. *Polymers* **2018**, *10*, 81. [CrossRef]
20. Donath, S.; Militz, H.; Mai, C. Wood modification with alkoxysilanes. *Wood Sci. Technol.* **2004**, *38*, 555–566. [CrossRef]
21. Broda, M.; Mazela, B.; Radka, K. Methyltrimethoxysilane as a stabilising agent for archaeological waterlogged wood differing in the degree of degradation. *J. Cult. Herit.* **2019**, *35*, 129–139. [CrossRef]
22. *GB/T1933-2009*; Method for Determination of the Density of Wood. National Standardization Administration: Beijing, China, 2009.
23. *GB/T 1931-2009*; Method for Determination of the Moisture Content of Wood. National Standardization Administration: Beijing, China, 2009.
24. *GB/T 1927.19-2021*; Test Methods for Physical and Mechanical Properties of Small Clear Wood Specimens—Part 19: Determination of Static Hardness. National Standardization Administration: Beijing, China, 2021.
25. Kang, S.M.; Cho, M.W.; Kim, K.M.; Kang, D.Y.; Koo, W.M.; Kim, K.H.; Lee, S.S. Cyproconazole impregnation into wood using sub-and supercritical carbon dioxide. *Wood Sci. Technol.* **2012**, *46*, 643–656. [CrossRef]
26. Chen, Z.; Dang, B.; Luo, X.; Li, W.; Li, J.; Yu, H.; Li, S. Deep eutectic solvent-assisted in situ wood delignification: A promising strategy to enhance the efficiency of wood-based solar steam generation devices. *ACS Appl. Mater. Interfaces* **2019**, *11*, 26032–26037. [CrossRef]
27. Cabrera-Alvarez, E.N.; Ramos-deValle, L.F.; Sánchez-Valdes, S.; Candia-García, A.; Soriano-Corral, F.; Ramírez-Vargas, E.; Patiño-Soto, P. Study of the silane modification of magnesium hydroxide and their effects on the flame retardant and tensile properties of high density polyethylene nanocomposites. *Polym. Compos.* **2014**, *35*, 1060–1069. [CrossRef]
28. Schorr, D.; Blanchet, P. Improvement of white spruce wood dimensional stability by organosilanes sol-gel imregnation and heat treatment. *Materials* **2020**, *13*, 973. [CrossRef]
29. Zheng, J.; Xu, X.; Yang, L. Dewatering characteristics of Juglans mandshurica wood using supercritical carbon dioxide: A comparison with conventional drying. *Dry. Technol.* **2024**, *42*, 926–935. [CrossRef]

30. Hafezi, S.M.; Doosthoseini, K. The influence of silane coupling agent and poplar particles on the wettability, surface roughness, and hardness of UF-bonded wheat straw (*Triticum aestivum* L.)/poplar wood particleboard. *J. For. Res.* **2014**, *25*, 667–670. [CrossRef]
31. Huang, G.H.; Chen, R.Y. Anatomical structure and contact angle of *Dalbergia latifolia* wood. *For. Eng.* **2023**, *39*, 85–91.
32. Liu, Y.; Liu, M.L.; Zhao, X.F.; Ren, W.B.; Wang, X.W.; Xu, G.F. Modification of Fast-growing Poplar by Ethyl Orthosilicate-KH-570 Composite Impregnation. *J. Beihua Univ. (Nat. Sci.)* **2020**, *21*, 416.
33. Popescu, C.M.; Broda, M. Interactions between different organosilicons and archaeological waterlogged wood evaluated by infrared spectroscopy. *Forests* **2021**, *12*, 268. [CrossRef]
34. Wang, C.; Mao, H.; Wang, C.; Fu, S. Dispersibility and hydrophobicity analysis of titanium dioxide nanoparticles grafted with silane coupling agent. *Ind. Eng. Chem. Res.* **2011**, *50*, 11930–11934. [CrossRef]
35. Parr, L.M.; Finzel, W.A. Water borne silicone alkyds and acrylics. *J. Water Borne Coat.* **1979**, *2*, 26–39.
36. Gogoi, R.; Tyagi, A.K. Surface modification of jute fabric by treating with silane coupling agent for reducing its moisture regain characteristics. *J. Nat. Fibers* **2021**, *18*, 803–812. [CrossRef]
37. Meekum, U.; Khongrit, A. Toughening of wood-plastic composites based on silane/peroxide macro crosslink poly (propylene) systems. *BioResources* **2018**, *13*, 1678–1695. [CrossRef]
38. Fathi, B.; Harirforoush, M.; Foruzanmehr, M.; Elkoun, S.; Robert, M. Effect of TEMPO oxidation of flax fibers on the grafting efficiency of silane coupling agents. *J. Mater. Sci.* **2017**, *52*, 10624–10636. [CrossRef]
39. Ouyang, L.; Huang, Y.; Cao, J. Hygroscopicity and characterization of wood fibers modified by alkoxysilanes with different chain lengths. *BioResources* **2014**, *9*, 7222–7233. [CrossRef]

Disclaimer/Publisher's Note: The statements, opinions and data contained in all publications are solely those of the individual author(s) and contributor(s) and not of MDPI and/or the editor(s). MDPI and/or the editor(s) disclaim responsibility for any injury to people or property resulting from any ideas, methods, instructions or products referred to in the content.